

Fig. S1. BCI treatment, immediately after MI, improves heart function and decreased cardiac fibrosis. (A) ECHO data showing ejection fraction and fractional shortening of sham-operated and 4 weeks post-MI rats treated with DMSO or BCI, which DMSO/BCI treatment was carried out immediately after MI (n = 8–9 per group). (B) Masson's trichrome staining and quantification of the Masson's trichrome-stained fibrotic area in sham, vehicle, and BCI-treated hearts at 28 days post-MI (Scale bar, 3 mm; n = 5 per group). Mean \pm s.e.m.; ns, not significant; *P < 0.05; **P < 0.01, ***P < 0.001.

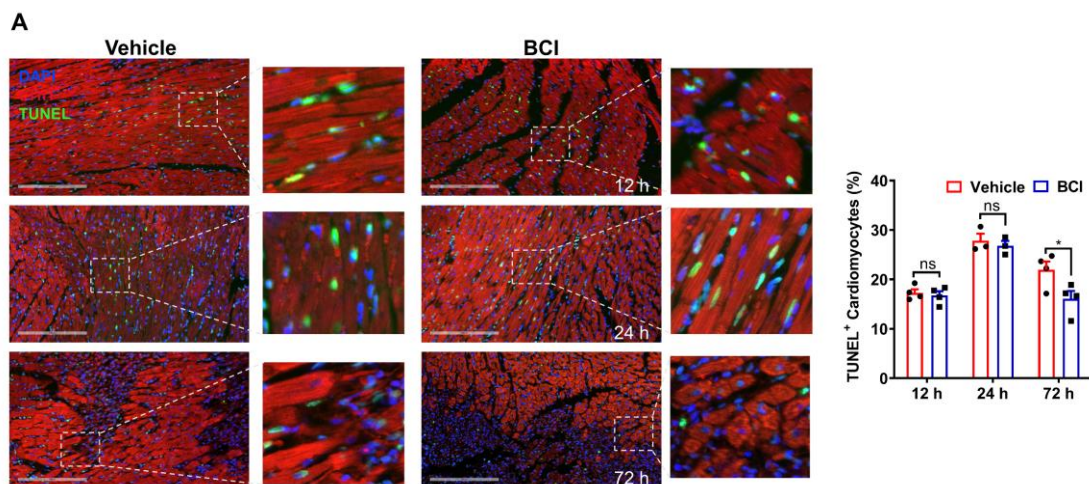


Fig. S2. BCI inhibits cardiomyocyte apoptosis at 72 h post MI, but not at 12 h and 24 h post MI. (A) Immunostaining and percentage of TUNEL-positive CMs in the infarcted zone of sham-operated, vehicle, and BCI-treated heart sections at 12 h, 24 h, and 72 h post-MI. Scale bars, 200 μ m. (n = 3–4 per group). Mean \pm s.e.m.; ns, not significant; *P < 0.05.

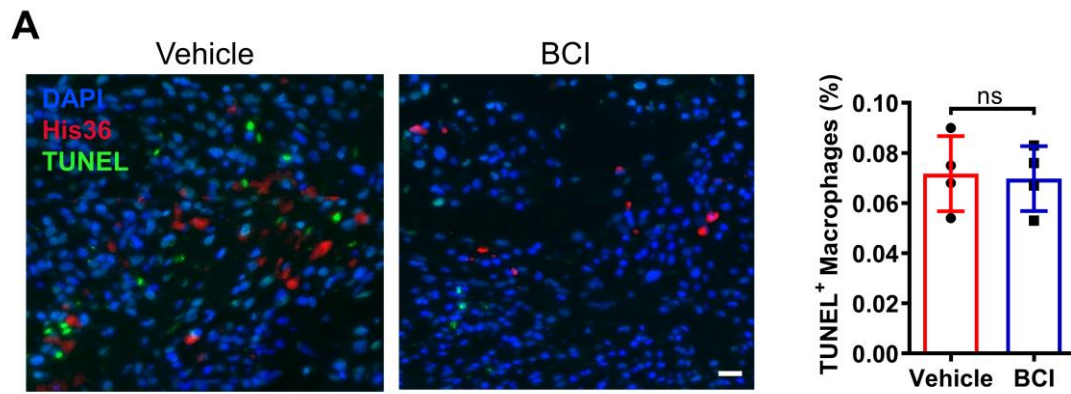


Fig. S3. BCI treatment has no effect on macrophage death of infarcted rat hearts at 7 days post MI. (A) Immunostaining and quantification of TUNEL-positive macrophages in the infarcted zone of vehicle and BCI-treated heart sections (Scale bar, 50 μ m; n = 4 per group). ns, not significant.

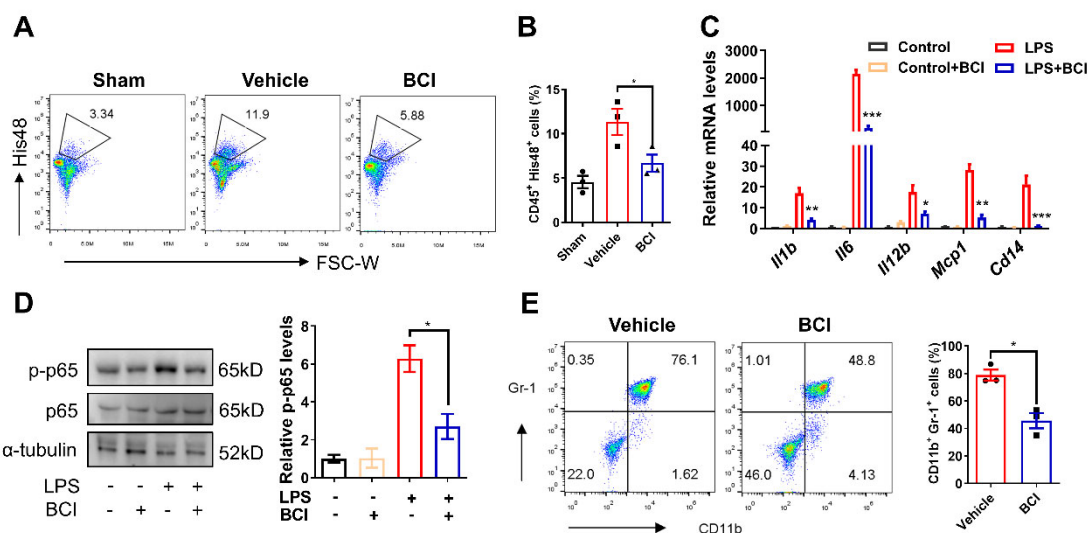


Fig. S4. BCI treatment inhibits neutrophil recruitment in infarcted rat hearts and LPS-induced mouse abdominal cells. (A, B) Percentages of His48⁺ neutrophils in the LV of rats at 7 days post-MI by flow cytometry (A), and statistics of His48⁺ neutrophils (B) (n = 3 per group and 2 hearts each group). (C) qRT-PCR showing expression levels of LPS-induced *Il1b*, *Il6*, *Il12b*, *Mcp1* and *Cd14* mRNAs in ABNs treated with DMSO or BCI (n = 3 per group). (D) Western blots and quantification of LPS-induced p-p65 and p65 in ABNs with DMSO or BCI (n = 3 per group). (E) Percentages of LPS-induced CD11b⁺ Gr-1⁺ neutrophils in mouse abdominal cells by flow cytometry, and statistics of CD11b⁺ Gr-1⁺ neutrophils (n = 3 per group and combined abdominal cells of 2 mice per sample). One-way ANOVA followed by Dunnett's multiple comparison test; mean ± s.e.m.; *P < 0.05; **P < 0.01, ***P < 0.001.

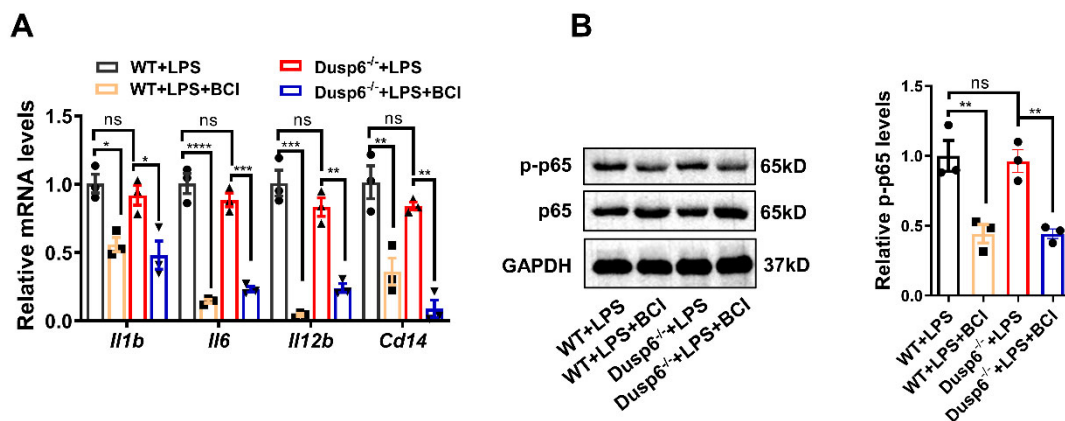


Fig. S5. BCI inhibits macrophage inflammation independent of DUSP6. (A) qRT-PCR showing expression levels of LPS-induced *Il1b*, *Il6*, *Il12b* and *Cd14* mRNAs in WT or *Dusp6*^{-/-} BMDMs with DMSO or BCI (n = 3 per group). (B) Western blots and quantification of LPS-induced p-p65 and p65 in WT or *Dusp6*^{-/-} BMDMs with DMSO or BCI (n = 3 per group). Mean ± s.e.m.; *P <0.05; **P <0.01, ***P <0.001, ****P <0.0001.

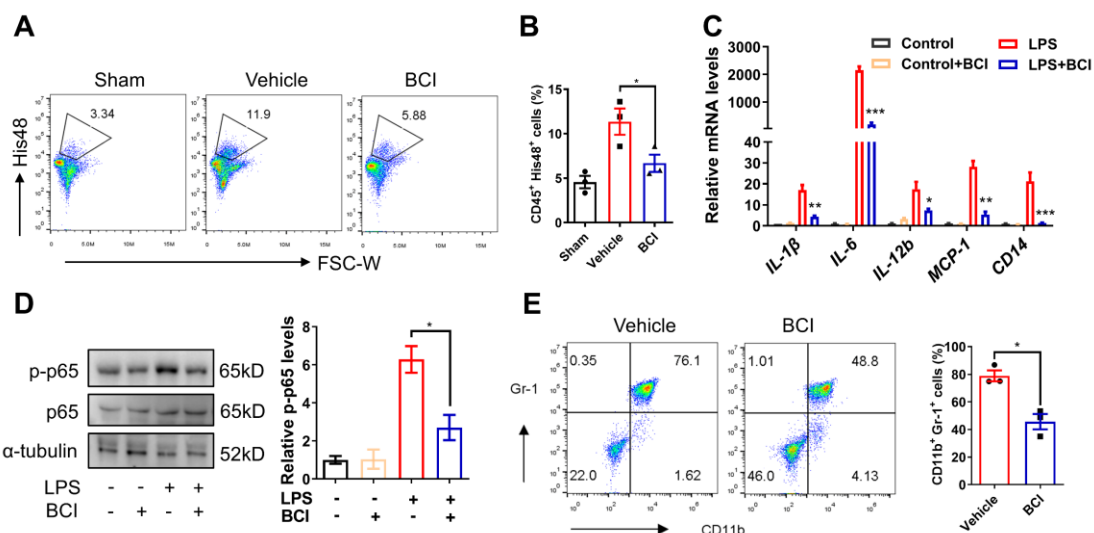


Fig. S4. BCI treatment inhibits neutrophil recruitment in infarcted rat hearts and LPS-induced mouse abdominal cells. (A, B) Percentages of His48⁺ neutrophils in the LV of rats at 7 days post-MI by flow cytometry (A), and statistics of His48⁺ neutrophils (B) (n = 3 per group and 2 hearts each group). (C) qRT-PCR showing expression levels of LPS-induced *IL-1 β* , *IL-6*, *IL-12b*, *Mcp1* and *CD14* mRNAs in ABNs treated with DMSO or BCI (n = 3 per group). (D) Western blots and quantification of LPS-induced p-p65 and p65 in ABNs with DMSO or BCI (n = 3 per group). (E) Percentages of LPS-induced CD11b⁺ Gr-1⁺ neutrophils in mouse abdominal cells by flow cytometry (G), and statistics of CD11b⁺ Gr-1⁺ neutrophils (H) (n = 3 per group and combined abdominal cells of 2 mice per sample). One-way ANOVA followed by Dunnett's multiple comparison test; Mean \pm s.e.m.; *P < 0.05; **P < 0.01, ***P < 0.001.

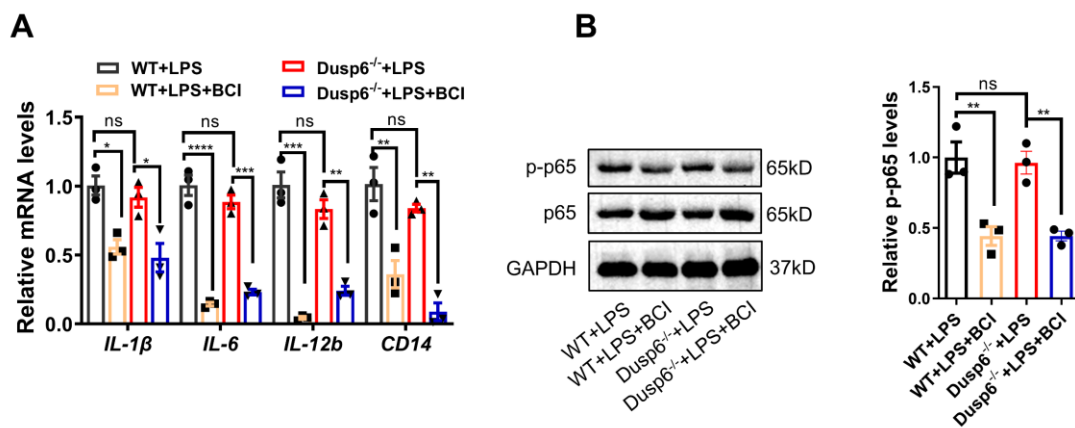


Fig. S5. BCI inhibits macrophage inflammation independent of DUSP6. (A) qRT-PCR showing expression levels of LPS-induced *IL-1 β* , *IL-6*, *IL-12b* and *CD14* mRNAs in WT or *Dusp6*^{-/-} BMDMs with DMSO or BCI (n = 3 per group). (B) Western blots and quantification of LPS-induced p-p65 and p65 in WT or *Dusp6*^{-/-} BMDMs with DMSO or BCI (n = 3 per group). Mean \pm s.e.m.; *P < 0.05; **P < 0.01, ***P < 0.001.

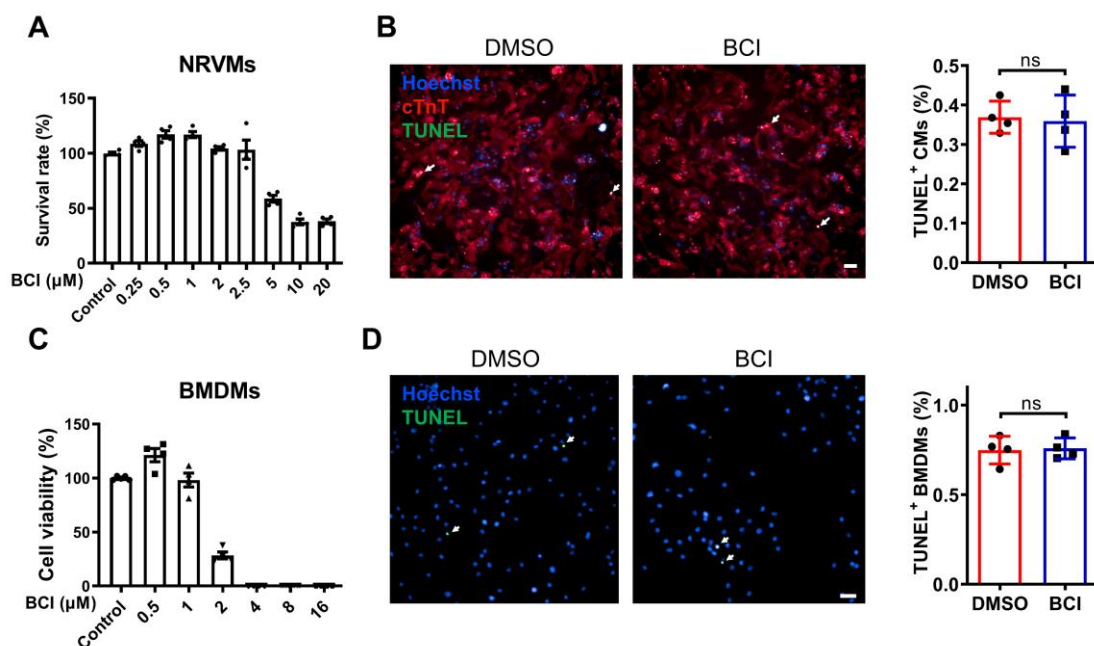


Fig. S6. Dose-dependent toxicity of BCI to NRVMs and BMDMs. (A) Cytotoxicity of different concentrations of BCI on NRVMs ($n = 4$ per group). (B) Immunostaining and statistics showing TUNEL-positive NRVMs after DMSO or $1 \mu\text{mol L}^{-1}$ BCI treatment. Scale bars, $50 \mu\text{m}$. ($n = 4$ per group). (C) Cytotoxicity of different concentrations of BCI on BMDMs ($n = 4$ per group). (D) Immunostaining and statistics showing TUNEL-positive BMDMs after DMSO or $1 \mu\text{mol L}^{-1}$ BCI-treated. Scale bars, $50 \mu\text{m}$. ($n = 4$ per group). ns, not significant.

Table S1. Primers used in real-time PCR analysis

Gene	Primer	Sequence (5'-3')
<i>Rat β-actin</i>	Forward	AACCTTCTTGCAGCTCCTCC
	Reverse	TACCCACCATCACACCCTGG
<i>Rat Inos</i>	Forward	TGAAGCACTTTGGGTGACCA
	Reverse	TATACACGGAAGGGCCAAGC
<i>Rat IL-1β</i>	Reverse	GACTTCACCATGGAACCCGT
	Forward	GGAGACTGCCCATTTCTCGAC
<i>Rat IL-6</i>	Forward	ACAAGTCCGGAGAGGAGACT
	Reverse	TTGCCATTGCACAACCTCTTTTC
<i>Rat IL-12b</i>	Forward	ATCATCAAACCGGACCCACC
	Reverse	CAGGAGTCAGGGTACTCCCA
<i>Rat Cd14</i>	Forward	TCAGAATCTACCGACCATGAAGC
	Reverse	GCTCCAGCCCAGTGAAAGAT
<i>Rat Mcp-1</i>	Forward	GATCCCAATGAGTCGGCTGG
	Reverse	ACAGAAGTGCTTGAGGTGGTT
<i>Rat Ccr2</i>	Forward	CAACCTGGCCATCTCTGACC
	Reverse	AAGTGCATGTCAACCACACAG
<i>Rat Ccl4</i>	Forward	GCTGTCAGCACCAATAGGCT
	Reverse	AGTTCCGATGAATCTTCCGGG
<i>Rat Cxcl9</i>	Forward	GACTCCAGCACGGTACTTA
	Reverse	ATGCAGGAGCATCGCTGATT
<i>Rat Mnda</i>	Forward	GGTGGGGAGTGGAAAATGGT
	Reverse	CGAGCTCTGGTGACCTTGAT
<i>Rat Egr1</i>	Forward	AACAACCCTACGAGCACCTG
	Reverse	AAAGGGGTTTCAGGCCACAAA
<i>Rat Grb2</i>	Forward	TTACGGAATCTCGCCGCTAC
	Reverse	AAAGGCTTCATGGGATGGGG
<i>Rat Retnla</i>	Forward	CTGGCAAGGTCCTGGAACT
	Reverse	GCATAGGCCCCAGTCAACGAT
<i>Rat Arg1</i>	Forward	GTGCCCTCTGTCTTTTAGGG
	Reverse	CAGACCGTGGGTTCTTCACA
<i>Rat Yml</i>	Forward	ATGAGATCCCCCAGCTGTCT
	Reverse	GGTTACGGTCACATGGGTGT